Supporting Information

Sander et al. 10.1073/pnas.1220512110

Relationship Between Raclopride and Dopamine Occupancies

Raclopride (RAC) competes with dopamine (DA) for binding to D2/D3 dopamine receptors (D2/D3R), such that increasing doses of RAC displace progressively more DA. To establish an approximate relationship between these occupancies, we assume transient equilibrium conditions, which are applicable at the peak response of RAC occupancy. Moreover, we assume that the nondisplaceable tissue-free fraction of [^{11}C]RAC stays constant. Because the onset rate constant is a function of the available receptor pool ($k_3 = k_{on}B_{max}$), the equilibrium condition can be written as (1)

$$(B_{max} - B_{DA} - B_{RAC})F_{DA} = K_{D,DA}B_{DA},$$

where

$$K_{D,DA} = \frac{k_{off,DA}}{k_{on,DA}},$$

or

$$\theta_{DA} = (1 - \theta_{RAC})\frac{F_{DA}}{F_{DA} + K_{D,DA}}, \qquad \textbf{[S1]}$$

with

$$\theta_{DA} = \frac{B_{DA}}{B_{max}} \quad \text{and} \quad \theta_{RAC} = \frac{B_{RAC}}{B_{max}}.$$

B_{max}, B_{DA}, and B_{RAC} refer to the total number of D2R receptors bound by DA and receptors bound by RAC, respectively. F_{DA} is the free DA concentration, $K_{D,DA}$ is the dissociation constant for DA at D2R, and fractional occupancies are denoted by θ_{DA} and θ_{RAC}. A solution for the free DA concentration should account both for displacement of bound DA into the free pool and for release of additional DA due to RAC binding presynaptic D2 autoreceptors. We assume the latter process occurs in proportion to RAC occupancy:

$$\begin{aligned} F_{DA} &= F_{DA}^{(0)} + B_{DA}^{(0)} - B_{DA} + \delta\theta_{RAC} \\ &= K_{D,DA}\frac{\theta_{DA}^{(0)}}{\left(1 - \theta_{DA}^{(0)}\right)} + B_{max}\left(\theta_{DA}^{(0)} - \theta_{DA}\right) + \delta\theta_{RAC}. \end{aligned} \qquad \textbf{[S2]}$$

We can employ Eqs. **S1** and **S2** to relate θ_{DA} and θ_{RAC} under several scenarios:

i) If we assume the free pool is large in comparison to the bound pool and we ignore RAC-induced DA release, this is equivalent to ignoring the second and third terms in Eq. **S2.** Under these conditions, the change in DA occupancy ($\Delta\theta_{DA} = \theta_{DA} - \theta_{DA}^{(0)}$) is proportional to RAC occupancy and DA occupancy, and we refer to this model as the linear approximation in the main text:

$$\Delta\theta_{DA} = -\theta_{RAC}\theta_{DA}^{(0)}. \qquad \textbf{[S3]}$$

ii) If we ignore RAC-induced DA release but conserve free plus bound dopamine by including the second term in **[S2]**, then the relationship in **[S3]** deviates only subtly from linearity using literature parameters (Fig. S5). Reported values for B_{max} in striatum for humans and nonhuman primates (NHPs) are about 20 nM (2, 3) and the $K_{D,DA}$ for D2R has been estimated to be about 100 nM (4). Although this model produces a relationship between RAC and DA occupancies that is not strictly linear, there is no meaningful difference between this model and the linear approximation.

iii) To include the effect of DA release due to antagonism of autoreceptors, we must rely upon data from rats, where i.p. injection of a dose slightly larger than the maximal dose used in this study produced an approximate doubling of extracellular DA (5). Under these conditions, the relationship between RAC and DA occupancies is described by a quadratic equation that deviates from linearity at middle occupancies (Fig. S5). This model produces a superlinear relationship between DA and RAC occupancies.

Negative changes in DA occupancy are plotted on the *y* axis in Fig. S5 to provide plots comparable to those in Fig. 5. The three curves correspond to the three assumptions above. Fitting a power function ($a(\theta_{RAC})^b$) to the superlinear relation that assumes additional DA release (Fig. S5, red curve), gives an exponent of $b = 1.6$. This value is very similar to experimental values we observed in Fig. 5. Thus, one interpretation of Fig. 5 is that a superlinear relationship between RAC occupancy and functional magnetic resonance imaging (fMRI) signal results from a superlinear relationship between RAC occupancy and changes in DA occupancy, together with a linear relationship between DA occupancy and the fMRI response.

Occupancy and Dynamic Binding Potential

Binding potential relative to a nondisplaceable tissue compartment (BP_{ND}) is defined in terms of the available concentration of receptors for binding (B_{avail}) relative to the dissociation constant (K_D), scaled by the fraction of ligand that is freely dissolved in tissue water (6). For this study, B_{avail} is equal to the total density of receptors (B_{max}) reduced by the fraction occupied by DA ($\theta_{DA} = B_{DA}/B_{max}$) and RAC ($\theta_{RAC}$). Consequently, the absolute change ΔBP_{ND}, relative to a tracer dose $BP_{ND}^{(0)}$, can be expressed in terms of occupancies:

$$\begin{aligned} \frac{\Delta BP_{ND}}{BP_{ND}^{(0)}} &= \frac{\left(1 - \theta_{DA}^{(0)}\right) - (1 - \theta_{DA} - \theta_{RAC})}{1 - \theta_{DA}^{(0)}} \\ &= \frac{\theta_{RAC} + \Delta\theta_{DA}}{1 - \theta_{DA}^{(0)}}. \end{aligned} \qquad \textbf{[S4]}$$

In all notations, θ denotes the theoretical occupancy of DA or RAC, whereas $\hat{\theta}$ denotes the measured occupancy value derived from positron-emission tomography (PET) imaging data. The superscript (0) denotes basal DA conditions. The change in DA occupancy can be related to RAC occupancy from Eq. **S3**, so that the fractional change in BP_{ND} becomes an index of RAC occupancy:

$$\hat{\theta}_{RAC} \equiv \frac{\Delta BP_{ND}}{BP_{ND}^{(0)}} \approx \theta_{RAC}. \qquad \textbf{[S5]}$$

All computations of BP_{ND} or the related "dynamic" binding potential (DBP_{ND}, Eq. **3**) were performed within the framework

of the simplified reference tissue model (SRTM) (7). In differential form, the time derivative of a tissue time-activity curve (TAC) ($\dot{C}_T$) can be written in terms of a reference region concentration (C_{REF}), an index (R_1) of the extraction-flow product relative to the reference region, a time constant for outflow from the reference region into plasma (k_2'), and the binding potential (BP_{ND}) as

$$\begin{aligned}\dot{C}_T &= R_1\dot{C}_{REF} + k_2 C_{REF} - k_{2a} C_T \\ &= R_1\dot{C}_{REF} + R_1 k_2' C_{REF} - \frac{R_1 k_2'}{1+BP_{ND}} C_T.\end{aligned} \quad \textbf{[S6]}$$

Although analytical solutions (7) or general linear model (GLM) techniques (8, 9) often solve for three local parameters, the reference region rate constant (k_2') is a global parameter, and thus Eq. **S4** contains an extra degree of freedom for each voxel or region of interest (ROI) (10). Two questions arise regarding the determination of an appropriate index of occupancy for comparison with a dynamic fMRI response like CBV(t):

i) Should we employ a steady-state analysis based upon BP_{ND}, even though physiology clearly is changing? BP_{ND} represents a weighted average across the 90-min measurement interval, and the weighting function changes vs. the injected mass dose. A dynamic index of receptor availability might offer a less biased alternative. A dynamic binding potential (DBP_{ND}, Eq. **3**) is a temporal analog of BP_{ND} that is determined in analysis by including a temporal dependence in parameter $k_{2a}(t)$ (8).

ii) Should we fix parameter k_2' or employ the original three-parameter SRTM? From inspection, it is clear that k_2' will be biased toward zero to reduce noise from the last two terms when BP is small, and this bias should affect other parameters as well. Because specific binding varies with mass dose, a three-parameter model may exhibit more bias vs. mass.

On the basis of this reasoning, we employed a standard steady-state BP_{ND} analysis with a two-parameter SRTM and a dynamic analysis by adding a time-dependent $k_{2a}(t)$ term. A comparison of the two model fits is shown in Fig. S2 for the 16 μg/kg dataset in animal M2. The dynamic analysis provides a better fit visually and is based on χ^2/DOF values, which are 2.8×10^6 and 0.7×10^6 for the SRTM and dynamic analysis, respectively.

Forward-Model Simulation and Analysis

This section describes simulations that (*i*) investigated the accuracy of SRTM estimates of occupancy using the coinfusion paradigm employed in this study and (*ii*) compared simplified estimates of specific binding based upon SRTM with actual specific binding in a simulation model with separate free and specifically bound compartments.

Because our experimental paradigm used progressively larger doses of RAC to reduce BP_{ND}, we investigated the accuracy of linear SRTM measurements of occupancy as a function of RAC dosage, using forward-model simulations, which included compartments for plasma, free, and specifically bound RAC and free and specifically bound DA (3). Literature values were employed for all rate constants, dissociation constants, and the concentration of D2R (Table S1). Plasma kinetics were approximated by a gamma-variate profile for RAC injection followed by biexponential decay of RAC from plasma; these kinetics were adjusted to match the reference region TAC from experimental data. Synthetic noise (11) was applied to TACs to approximate experimental data from basal ganglia ROIs. Because simulations separated free and specifically bound compartments, true values for specific binding were known as a function of time. Hence, we could assess the accuracy of SRTM analyses based upon BP_{ND} values vs. that based on time-dependent binding models.

We analyzed simulated data by the GLM, using the same software that was employed to analyze real data. Analyses used the integral form of **[S6]** and either three local constant parameters (8), as in **[S6]**, or two local parameters (12). Additionally, we evaluated the effect of a time-dependent k_{2a} (following ref. 8). The time dependence was implemented as a gamma-variate function specified by a single parameter defining the time to peak (τ). Thus, SRTM included either three or four local parameters, and the reduced model [multilinear reference tissue model (MRTM2)] included a global value for k_2' ($k_{2,G}'$) and either two or three local parameters, with the latter version explicitly formulated as

$$\begin{aligned}C_T(t) = R_1\left(C_{REF} + k_{2,G}'\int C_{REF}(t)dt\right) \\ -k_{2a}\int C_T(t)dt - k_{2a\gamma}\int \gamma(t,\tau)C_T(t)dt,\end{aligned} \quad \textbf{[S7]}$$

where

$$\gamma(t,\tau) = (t/\tau)e^{(1-t/\tau)}.$$

When employing a time-dependent k_{2a} term, the time-to-peak parameter was determined in two different ways to determine the sensitivity of results to the choice of the time constant τ: (*i*) by minimizing the χ^2/DOF of the GLM fit to data for each dose or (*ii*) by minimizing the χ^2/DOF for the lowest dose and maintaining that value of τ for all doses.

The main simulation results are summarized in Fig. S3. The conventional SRTM model produced estimates of RAC occupancies that underestimated true peak occupancies by 10–15% at high doses (black squares). Best results were obtained by adding a gamma time dependence to MRTM2 (red circles) in which the variable τ was optimized for each dose. Errors in occupancy were <2% at all doses. Intermediate results with up to 7% error were obtained by using fixed values of τ, based upon fits within MRTM2 for data at the lowest mass dose. Fitting up to four parameters (SRTM with a gamma time dependence on k_{2a}) did not provide stable estimates of τ across doses within simulations.

These results suggest that the most accurate method for determining peak changes in RAC occupancies in this coinfusion paradigm is to (*i*) fit parameter k_2' in a high-binding region (e.g., putamen) at low mass dose, (*ii*) eliminate the extra degree of freedom incorporated into the three-parameter SRTM model by fixing k_2', and (*iii*) add a time-dependent binding term that is optimized at each dose by minimizing the χ^2/DOF in a high-binding region (e.g., putamen).

In a full reference tissue model (FRTM) (13), specific binding is known, whereas SRTM analysis determines only the ratio of the rate constants (k_3, k_4) between the free and specifically bound compartments, as well as an effective rate constant (k_{2a}) for washout. In measurements and fits, the offset rate constant (k_4) has been determined to be about 3–10 times smaller than the washout rate constant (3, 14), so that the free and nonspecifically bound compartment changes much more rapidly in time than the specifically bound compartment. Thus, an approximate index of specific binding can be obtained through SRTM by correcting the tissue concentration TAC for ligand delivery and washout by subtracting the reference region and scaling for the relative flow-extraction product (R_1) as $C_S \approx \hat{S} = C_T - R_1 C_{REF}$. Fig. S4 compares specific binding C_S as determined from an analysis with the FRTM to the specific binding estimate $\hat{S}$. In both cases, the peak of $\hat{S}$ is shifted by no more than a few minutes compared to that of C_S, which is comparable to the uncertainty in the time-to-peak response of fMRI signal and PET-specific binding in this study based upon optimization of the χ^2/DOF, as described in *Results*.

1. Slifstein M, Laruelle M (2001) Models and methods for derivation of in vivo neuroreceptor parameters with PET and SPECT reversible radiotracers. *Nucl Med Biol* 28(5):595–608.
2. Cumming P (2011) Absolute abundances and affinity states of dopamine receptors in mammalian brain: A review. *Synapse* 65(9):892–909.
3. Endres CJ, et al. (1997) Kinetic modeling of [11C]raclopride: Combined PET-microdialysis studies. *J Cereb Blood Flow Metab* 17(9):932–942.
4. Fisher RE, Morris ED, Alpert NM, Fischman AJ (1995) In vivo imaging of neuromodulatory synaptic transmission using PET: A review of relevant neurophysiology. *Hum Brain Mapp* 3:24–34.
5. Hertel P, Fagerquist MV, Svensson TH (1999) Enhanced cortical dopamine output and antipsychotic-like effects of raclopride by alpha2 adrenoceptor blockade. *Science* 286(5437):105–107.
6. Innis RB, et al. (2007) Consensus nomenclature for in vivo imaging of reversibly binding radioligands. *J Cereb Blood Flow Metab* 27(9):1533–1539.
7. Lammertsma AA, Hume SP (1996) Simplified reference tissue model for PET receptor studies. *Neuroimage* 4(3 Pt 1):153–158.
8. Alpert NM, Badgaiyan RD, Livni E, Fischman AJ (2003) A novel method for noninvasive detection of neuromodulatory changes in specific neurotransmitter systems. *Neuroimage* 19(3):1049–1060.
9. Zhou Y, Endres CJ, Brasić JR, Huang SC, Wong DF (2003) Linear regression with spatial constraint to generate parametric images of ligand-receptor dynamic PET studies with a simplified reference tissue model. *Neuroimage* 18(4):975–989.
10. Wu Y, Carson RE (2002) Noise reduction in the simplified reference tissue model for neuroreceptor functional imaging. *J Cereb Blood Flow Metab* 22(12):1440–1452.
11. Logan J, et al. (2001) A strategy for removing the bias in the graphical analysis method. *J Cereb Blood Flow Metab* 21(3):307–320.
12. Ichise M, et al. (2003) Linearized reference tissue parametric imaging methods: Application to [11C]DASB positron emission tomography studies of the serotonin transporter in human brain. *J Cereb Blood Flow Metab* 23(9):1096–1112.
13. Lammertsma AA, et al. (1996) Comparison of methods for analysis of clinical [11C] raclopride studies. *J Cereb Blood Flow Metab* 16(1):42–52.
14. Kapur S, Seeman P (2000) Antipsychotic agents differ in how fast they come off the dopamine D2 receptors. Implications for atypical antipsychotic action. *J Psychiatry Neurosci* 25(2):161–166.

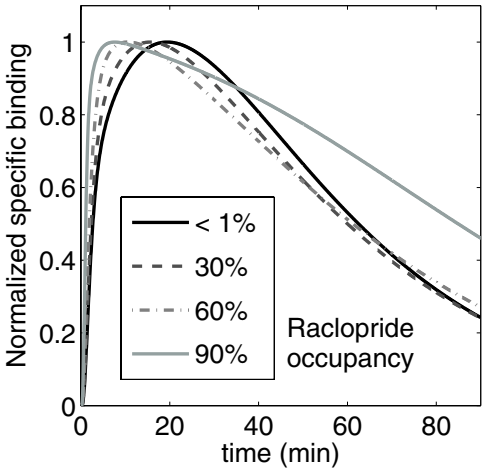

Fig. S1. Simulations of a multicompartmental model based upon first-order kinetics: Specific binding of raclopride vs. time and for increasing dose, normalized to the maximum value to observe differences in shape due to receptor saturation.

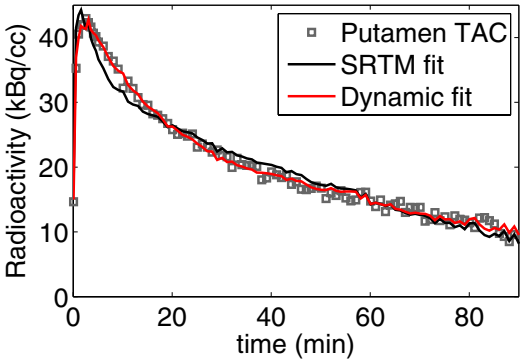

Fig. S2. Comparison of an SRTM fit (black line) with a dynamic fit (red line) that allows the use of DBP_{ND} (for the 16 μg/kg RAC mass dose in M2). The dynamic method shows an improved fit visually and by χ^2/DOF measures.

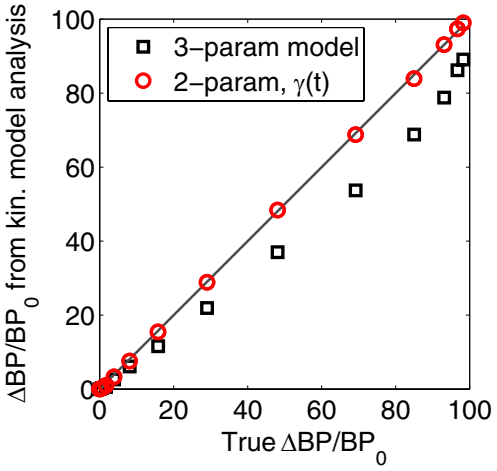

Fig. S3. Analysis of simulated data to determine the accuracy of occupancy estimates relative to true peak change in occupancy. Simulations were analyzed within the SRTM framework by GLM: Conventional three-parameter SRTM analyses with a fixed BP_{ND} (black squares) systematically underestimate peak occupancy, whereas the two-parameter SRTM (red circles) accurately determines peak occupancy when a gamma-variate function is embedded in parameter k_{2a}.

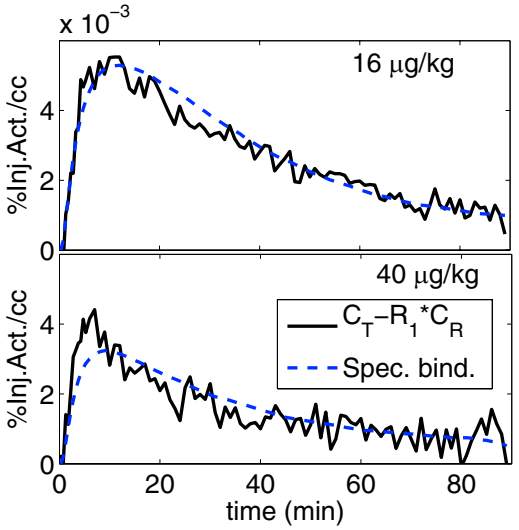

Fig. S4. Estimate of specific binding computed from the data ($\hat{S} = C_T - R_1 C_{REF}$, solid black line) compared with specific binding (dashed blue line) modeled with a full reference tissue model based on fitted parameters for the two highest RAC mass doses in M1 (16 μg/kg and 40 μg/kg).

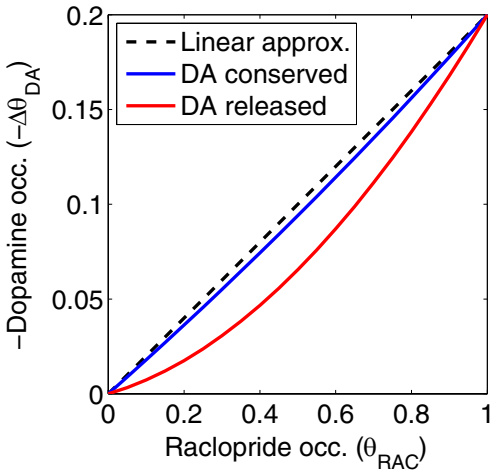

Fig. S5. Relationship between the fractional occupancies of raclopride (θ_{RAC}) and the change in fractional occupancy of DA ($\Delta\theta_{DA}$), which drives the fMRI signal, using the linear approximation of Eq. **S3** (dashed black line) or estimating effects of DA displacement (solid blue line) and displacement plus release (solid red line). Calculations assume a 20% basal DA occupancy.

Table S1. Parameters used in forward-model simulations

Parameter	Value	Species	Source or reference
B_{max}	17 nM	NHP	Endres et al. (1997) (1)
K_D	3.8 nM	Human	Farde et al. (1986) (2)
θ_{DA} in basal state	25%	Human	Verhoeff et al. (2002) (3)
BP_{ND}	3.36	NHP	From B_{max}, K_D, and θ_{DA}
K_1'	0.17 min^{-1}	NHP	Endres et al. (1997) (1)
V_D, distribution volume in reference region	0.7	NHP	Endres et al. (1997) (1)
$R_1 = K_1/K_1' = k_2/k_2'$	0.8	NHP	Measured from data
$K_{D,DA}$	100 nM	Human	Fisher et al. (1995) (4)
$k_{4,DA} = k_{off,DA}$	1 min^{-1}	NHP	Logan et al. (2001) (5)
$k_4 = k_{off,RAC}$	0.07 min^{-1}	NHP	Endres et al. (1997) (1)

1. Endres CJ, et al. (1997) Kinetic modeling of [11C]raclopride: combined PET-microdialysis studies. *J Cereb Blood Flow Metab* 17(9):932–942.
2. Farde L, Hall H, Ehrin E, Sedvall G (1986) Quantitative analysis of D2 dopamine receptor binding in the living human brain by PET. *Science* 231(4735):258–261.
3. Verhoeff NPLG et al. (2002) Dopamine depletion results in increased neostriatal D(2), but not D(1), receptor binding in humans. Mol Psychiatry 7:233, 322328.
4. Fisher RE, Morris ED, Alpert NM, Fischman AJ (1995) In vivo imaging of neuromodulatory synaptic transmission using PET: a review of relevant neurophysiology. *Hum Brain Mapp* 3:2434.
5. Logan J, et al. (2001) A strategy for removing the bias in the graphical analysis method. *J Cereb Blood Flow Metab* 21(3):307–320.